FULL PAPER

Dalton
www.rsc.org/dalton

Heterobimetallic Pt(II)–M(I) (M = Cu, Ag) eight-membered macrocyclic complexes with large-bite P,N-ligand bridges†

Qing-Shan Li,* Feng-Bo Xu, Da-Jun Cui, Kai Yu, Xian-Shun Zeng, Xue-Bing Leng, Hai-Bin Song and Zheng-Zhi Zhang*

State Key Laboratory of Elemento-Organic Chemistry, Nankai University, Tianjin 300071, P. R. China. E-mail: zzzhang@public.tpt.tj.cn; qli@nankai.edu.cn

Received 14th November 2002, Accepted 24th February 2003
First published as an Advance Article on the web 13th March 2003

Reaction of a new large-bite P,N-ligand, 2-(*N*-diphenylphosphinomethyl-*N*-benzyl)aminopyridine (**1**) with (COD)PtCl$_2$ and (COD)Pt(C≡CPh)$_2$ give *cis*-(L)$_2$PtCl$_2$ (**2**) and *trans*-(L)$_2$Pt(C≡CPh)$_2$ (**3**), respectively. Complex **3** reacted with M(I) (M = Cu, Ag) perchlorate using its pyridyl and alkynyl groups to afford a novel type of mixed-metal macrocyclic complexes PtM$_2$(L)$_2$(C≡CPh)$_2$(ClO$_4$)$_2$ (M = Cu, **4**; M = Ag, **5**). Complex **4** can be converted to the solvated complexes Pt[Cu(solvent)]$_2$(μ-L)$_2$(C≡CPh)$_2$(ClO$_4$)$_2$ (solvent = H$_2$O, **4**; CH$_3$CN, **4″**) by recrystallization of **4** in the corresponding solvents. The crystal structures of complexes **2**, **3**, **4** and **4″**·CH$_2$Cl$_2$ and luminescence properties of **3**, **4** and **5** have been determined.

Introduction

Although binuclear complexes bridged by some rigid hemilabile ligands such as (2-diphenylphosphine)pyridine[1] and 2,6-bis(diphenylphosphino)pyridine[2] possess novel structures and have extensively been studied, they are lacking in reactivity owing to the limitation of their rigid structural frameworks. Current attention has been focused on the coordination chemistry of P–N non-rigid hemilabile ligands, but they usually display P–N chelating cyclization modes to transition metals. A few examples show P,N-bridging coordination modes to some homobimetals.[3] Recently we have devoted our efforts to studies on synthetic methods, chemical and physical properties of binuclear complexes bridged by some non-rigid hemilabile ligands.[4] Herein we report on the synthesis and photophysical properties of two novel heterobimetallic (Pt–Cu and Pt–Ag) eight-membered macrocycle complexes bridged by a new P,N-ligand, 2-(*N*-diphenylphosphinomethyl-*N*-benzyl)aminopyridine (L). Until now, to our best knowledge, there are no examples of such eight-membered macrocyclic heterobimetallic complexes bridged by a large-bite P,N-ligand in the literature.

Results and discussion

As shown in Scheme 1, the new large-bite P,N-ligand, 2-(*N*-diphenylphosphinomethyl-*N*-benzyl)aminopyridine (L), **1**, was easily prepared by the reaction of 2-(*N*-benzyl)aminopyridine with Ph$_2$PH and (HCHO)$_n$, using a developed method of the Mannich reaction in acidic medium.[4c] Reaction of **1** with (COD)Pt(C≡CPh)$_2$ gives *cis*-P-coordinated (L)$_2$PtCl$_2$, **2**, with no *trans*-product being formed. Complex **2** reacted with NaC≡CPh to afford *trans*-(L)$_2$Pt(C≡CPh)$_2$, **3**. Apparently the orientation of the two P atoms of the ligand in square planar configuration around the Pt atom is converted from *cis*- in **2** to *trans*-form in **3** in this process, and the pyridyl N atom of the ligand remains uncoordinated. Complex **3** can also be prepared more conveniently and in higher yield (85%) by the reaction of ligand **1** with the complex (COD)Pt(C≡CPh)$_2$. Complex **3** with a *trans*-P configuration readily reacts with metal ions using its pyridyl N and alkynyl group. In the preparation of the mixed-metal macrocyclic complexes **4** and **5**, the reaction mixture immediately turned to a pale-yellow or yellow solution upon addition of white copper(I) or silver(I) perchlorate to a colorless solution of **3** in CH$_2$Cl$_2$, indicating a fast reaction rate. After work-up the product was obtained in high yield. When complexes **4** and **5** reacted with Na$_2$S in CH$_3$OH, the coordinated Cu or Ag atom could be removed from the trinuclear complexes, and complex **3** can be recovered quantitatively (Scheme 1). All the complexes show satisfactory elemental analysis and have been characterized by FT-IR, ^{1}H NMR and ^{31}P NMR spectroscopy, and complex **5** has also been measured by FAB-MS. Furthermore, complexes **2**, **3**, **4′** and **4″**·CH$_2$Cl$_2$ were determined by X-ray single crystal analysis. It is noteworthy that in complexes **4** and **5**, the alkynyl anions were bonded to different metal ions in the μ-η^1,η^2-mode and thus two eight-membered bimetallomacrocycles were formed in one molecule by the cyclization of the large-bite P,N-ligand to different metal ions.

Interestingly, although bimetallic complex **4** was an air-stable compound, because of the coordinated unsaturation of Cu ions, **4** can be converted to new solvent coordinated complexes Pt[Cu(H$_2$O)]$_2$(μ-L)$_2$(C≡CPh)$_2$(ClO$_4$)$_2$ (**4′**) and Pt[Cu(CH$_3$CN)]$_2$-(μ-L)$_2$(C≡CPh)$_2$(ClO$_4$)$_2$ (**4″**), upon recrystallization of **4** from CH$_2$Cl$_2$–wet MeOH and CH$_2$Cl$_2$–CH$_3$CN, respectively. On the other hand, when heating or under reduced pressure, both complexes **4′** and **4″** lose their coordinated solvents H$_2$O or MeCN to reform the original heterometallic complex **4** with the mixed-metal macrocycle framework remaining intact, as shown in Scheme 2.

Figs. 1–4 depict the perspective drawings of **2**, **3** and the complex cations of **4′**, **4″**·CH$_2$Cl$_2$, respectively, with atomic numbering. The crystal data and refinement parameters as well as selected bond distances and bond angles of these complexes are collected in Tables 1 and 2, respectively. From these data, it can be concluded that all the complexes **3**, **4′** and **4″**·CH$_2$Cl$_2$ have a square planar configuration of Pt(II) with both P atoms and alkynyl groups in *trans*-positions, respectively. However, in complex **2** the platinum atom exhibits a severely distorted square planar coordination geometry [bond angles, P(1)–Pt(1)–P(1A) 97.78; P(1)–Pt(1)–Cl(1A) 88.13(14); P(1A)–Pt(1)–Cl(1) 88.13(14); Cl(1A)–Pt(1)–Cl(1) 87.4(2)], due to the interaction of the two large ligands **1** in *cis*-positions of the Pt atom. In complexes **2** and **3**, the free pyridyl groups of the ligands **1** are located in the opposite orientation in their crystal structures, but in mixed-metal complexes **4′** and **4″**·CH$_2$Cl$_2$, each pyridyl group and the alkynyl group chelate to a Cu(I) atom, forming two mixed-metal macrocycles in one molecule. In addition, one solvent molecule was attached on each of the Cu atoms. Each copper atom in **4′** and **4″**·CH$_2$Cl$_2$ is two coordinate with a

---

† Electronic supplementary information (ESI) available: UV-vis absorption spectra and the fluorescence excitation and emission spectra of complexes **3** and **5**. See http://www.rsc.org/suppdata/dt/b2/b211301p/

DOI: 10.1039/b211301p

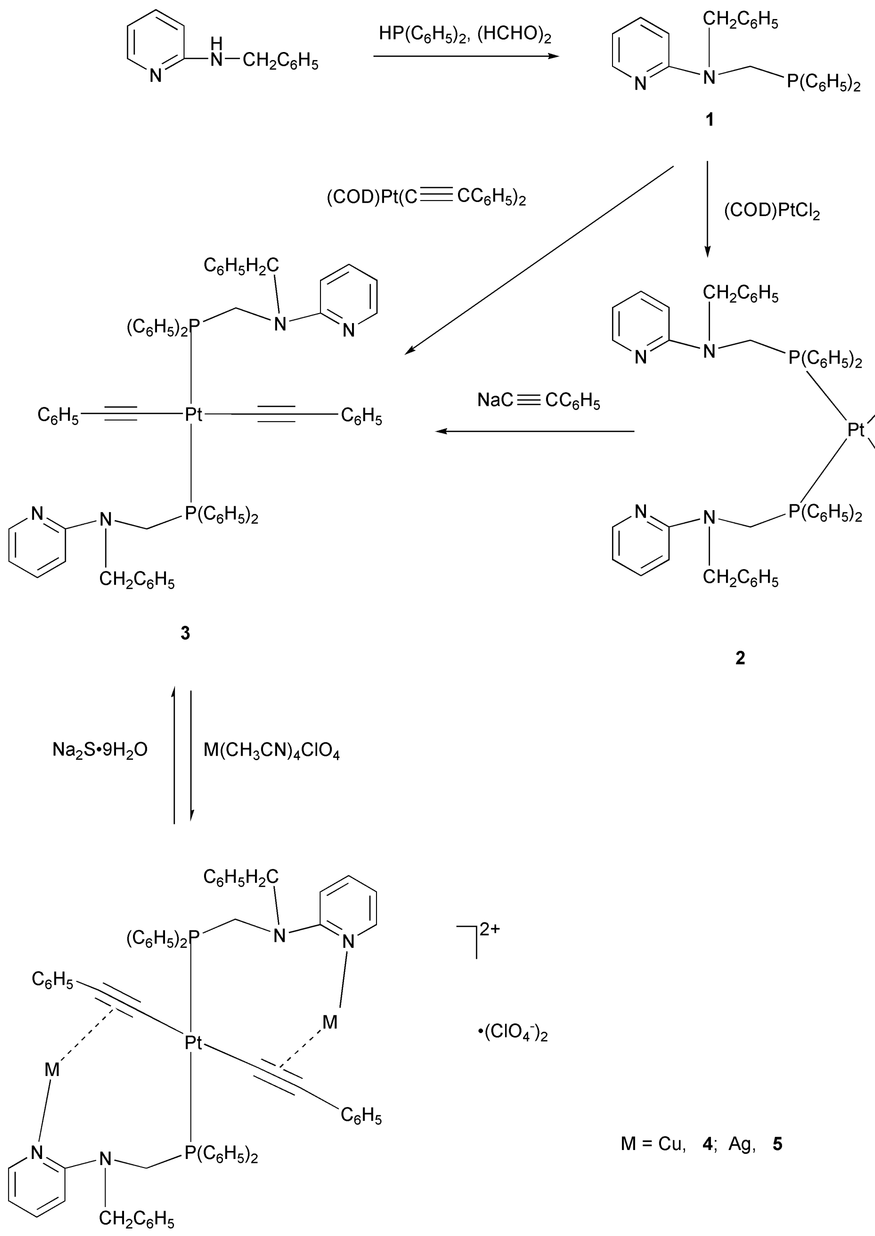

Scheme 1

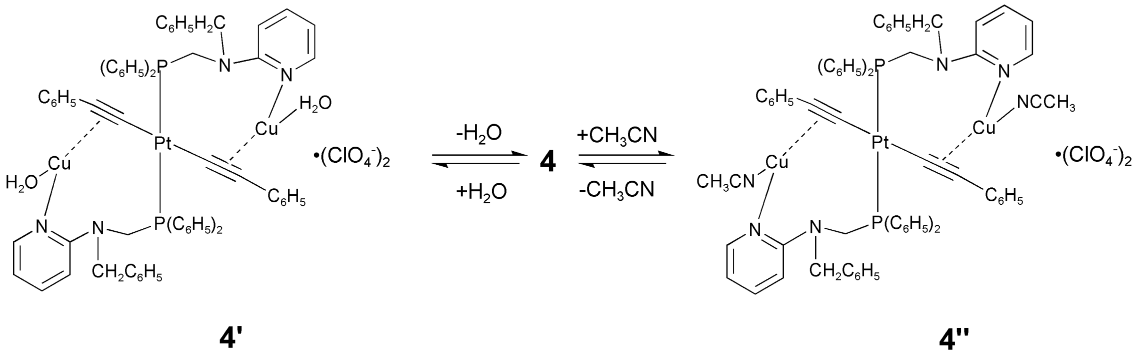

Scheme 2

bonding interaction to the centre of the C–C acetylenic bond, while the coordination geometry of platinum atom is approximate square planar.

Comparison of some bond distances and bond angles in **3**, **4′** and **4″**·CH_2Cl_2 with those in Pt–Cu complexes with similar structure, $[Pt_2(\mu\text{-dppm})_2(C{\equiv}CPh)_4\{Cu(CH_3CN)\}_2]^{2+}$ (**A**),[5] $[Pt(\mu\text{-dppy})_2(C{\equiv}CPh)_2\{Cu(CH_3CN)_2\}_2]^{2+}$ (**B**),[6] $[Pt(bipy)(C{\equiv}CPh)_2CuBr]$ (**C**)[7] and $[Pt(^tBu_2bipy)(C{\equiv}CC_6H_4Me\text{-}p)_2Cu(SCN)]$ (**D**)[8] are summarized in Table 3. As shown in Table 3, the Cu–C_1 and Cu–C_2 bond distances and the C_1–C_2–C_3 bond angles (–C≡C–Ph angles) in complexes **4′** and **4″**·CH_2Cl_2 are obviously shorter and less than those found in complexes **A**–**D**, respectively, which indicate that there are stronger interactions between Cu and the alkynyl groups in complexes **4′** and **4″**·CH_2Cl_2.

The electronic absorption spectra of the trinuclear complexes **4** (Fig. 5) and **5** show similar patterns with low-lying bands at

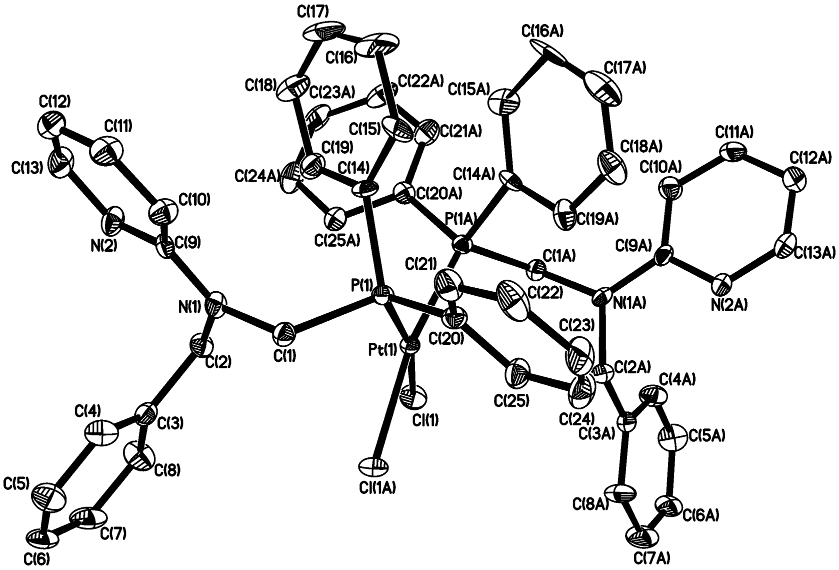

Fig. 1 Perspective drawing of **2** with atomic numbering scheme. Hydrogen atoms have been omitted for clarity. Thermal ellipsoids are shown at the 30% probability level.

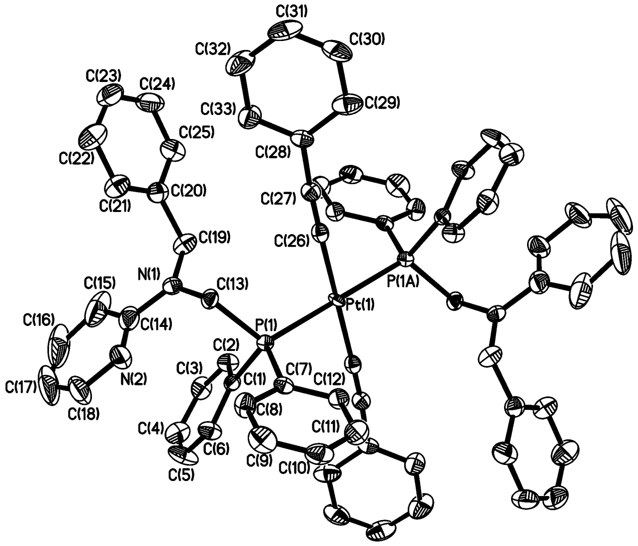

Fig. 2 Perspective drawing of **3** with atomic numbering scheme. Hydrogen atoms have been omitted for clarity. Thermal ellipsoids are shown at the 30% probability level.

ca. 323 and 319 nm, respectively, similar to that observed for the mononuclear complex **3** with a band at about 312 nm (Table 4). With reference to previous spectroscopic studies[5,6,9] on the similar structural complexes, the band at *ca.* 320 nm is assigned to a metal-to-ligand charge transfer (MLCT) [5d(Pt) ⟶ π*(PhC≡C⁻)] transition and the transition is likely to have some intraligand (IL) character [π(PhC≡C⁻) ⟶ π*(PhC≡C⁻), ILCT] mixed into it.

The photophysical data of **3**–**5** are summarized in Table 4. Upon photoexcitation at $\lambda > 300$ nm, **4** and **5** exhibit two fluorescence emission bands in CH_2Cl_2 solution (1×10^{-5} M) at room temperature, at about 400 and 730 nm, respectively. Compared with the emission spectra of complexes **A** and **B**,[5,6,9] because of the large energy difference between the two bands, the higher energy emission bands (408 and 385 nm) observed in **4** and **5** are tentatively assigned as ^{3}MLCT/IL (intraligand phosphorescence of the bridging diphosphine ligands), similar to that of the mononuclear complex **3** in 408 nm. The low-energy emission bands at *ca.* 730 nm in a very broad range are proposed to arise from Pt ··· Cu(Ag) interactions. The observation of the red emission bands at *ca.* 730 nm in CH_2Cl_2 suggests that the Pt ··· Cu(Ag) interaction is much stronger than that in CH_2Cl_2 solutions of complexes **A** and **B**.

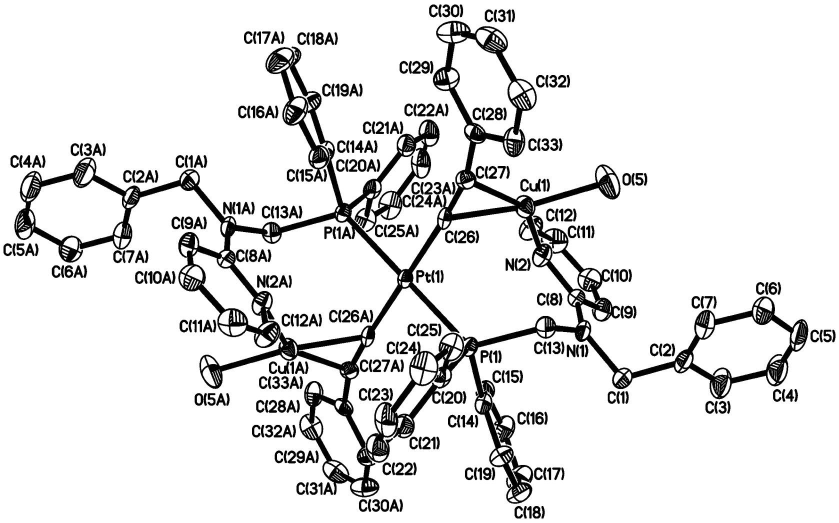

Fig. 3 Perspective drawing of the cation in **4′** with atomic numbering scheme. Hydrogen atoms are located for the water molecules in compound **4′** and the others have been omitted for clarity. Thermal ellipsoids are shown at the 30% probability level.

Table 1 Crystal data and refinement parameters

	2	**3**	**4′**	**4″·CH$_2$Cl$_2$**
Formula	$C_{50}H_{46}N_4P_2PtCl_2$	$C_{66}H_{56}N_4P_2Pt$	$C_{66}H_{60}Cl_2Cu_2N_4O_{10}P_2Pt$	$C_{71}H_{64}Cl_4Cu_2N_6O_8P_2Pt$
M_w	1030.84	1162.18	1524.19	1655.26
Crystal system	Orthorhombic	Monoclinic	Triclinic	Monoclinic
Space group	$Fdd2$	$P2_1/c$	$P\bar{1}$	$P2_1/c$
a/Å	19.399(10)	9.3607(9)	10.585(4)	12.274(4)
b/Å	41.78(2)	10.6329(10)	12.007(4)	19.011(6)
c/Å	10.915(5)	27.735(3)	13.292(5)	16.666(5)
α/°	90	90	108.946(6)	90
β/°	90	95.618(2)	97.064(5)	92.685(5)
γ/°	90	90	98.108(6)	90
V/Å^3	8847(8)	2747.2(5)	1555.9(9)	3884(2)
Z	8	2	1	2
D_c/g cm^{-3}	1.548	1.405	1.627	1.417
μ/mm^{-1}	3.405	2.657	3.119	2.571
F(000)	4128	1176	764	1664
Crystal size/mm	0.15 × 0.10 × 0.05	0.30 × 0.25 × 0.01	0.20 × 0.20 × 0.06	0.44 × 0.38 × 0.32
λ/Å	0.71073	0.71073	0.71073	0.71073
θ_{min}, θ_{max}/°	1.95, 25.03	1.48, 25.39	1.65, 23.34	1.98, 26.38
T/K	293(2)	293(2)	293(2)	293(2)
No. of data collected	8907	5835	4708	22034
No. of unique data	3599	2664	4275	7926
R_{int}	0.0728	0.0369	0.0254	0.0531
No. of refined params.	267	359	394	427
GOF on F^2 [a]	1.020	1.149	1.071	1.160
Final R indices [b]				
$R1$	0.0565	0.0242	0.0429	0.0686
$wR2$	0.1369	0.0555	0.0910	0.1698
R indices (all data)				
$R1$	0.0741	0.0255	0.0559	0.1115
$wR2$	0.1466	0.0732	0.1068	0.1896
Final diff. map/e Å^{-3}	1.800, −2.515	1.206, −0.847	1.360, −1.336	1.407, −0.776
Refinement method	Full-matrix least-squares on F^2			

[a] GOF = $[\Sigma w(F_o^2 - F_c^2)^2/(n - p)]^{1/2}$, where n is the number of reflections and p is the number of parameters refined. [b] $R1 = \Sigma(||F_o| - |F_c||)/\Sigma|F_o|$; $wR2 = 1/[\sigma^2(F_o^2) + (0.0691P) + 1.4100P]$ where $P = (F_o^2 + 2F_c^2)/3$.

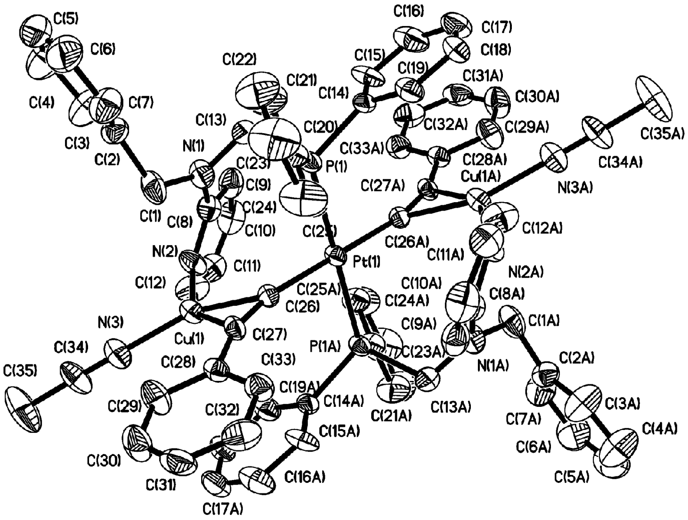

Fig. 4 Perspective drawing of the cation in **4″**·CH$_2$Cl$_2$ with atomic numbering scheme. Hydrogen atoms have been omitted for clarity. Thermal ellipsoids are shown at the 30% probability level.

Experimental

All the reactions were carried out under a prepurified nitrogen atmosphere using standard Schlenk or vacuum line techniques. The solvents were purified by standard methods. [2-(*N*-benzyl)-amino]pyridine,[10] (COD)PtCl$_2$,[11] (COD)Pt(C≡CPh)$_2$ [12] were prepared according to the literature methods. FT-IR spectra were measured on a Bruker FT-IR Equinox-55 infrared spectrophotometer; ^{1}H NMR and ^{31}P{^{1}H} NMR spectra were recorded on Bruker AC-200 NMR spectrometer using CDCl$_3$ as solvent. Elemental analyses were performed by a Yanaco MT-3 analyzer. Mass spectra were recorded on a VG ZAB-HS spectrometer. X-Ray crystallographic data were performed on a Bruker Smart 1000 instrument. The luminescence spectra and UV-absorption spectra were conducted on Perkin-Elmer LS-50B luminescence spectrometer and Shimadzu UV-1601PC UV-visible spectrophotometer in CH$_2$Cl$_2$ solution (concentration, 1 × 10^{-5} M), respectively. Melting points were determined on a Yanaco micromelting point apparatus MP-500.

CAUTION: While none of these perchlorate complexes has proved to be shock sensitive,[13] nevertheless proper care should always be taken.

Preparation of the ligand, 2-(*N*-diphenylphosphinomethyl-*N*-benzyl)aminopyridine (1)

To a solution of 2-(*N*-benzyl)aminopyridine (3.68 g, 20 mmol), paraformaldehyde (0.75 g, 25 mmol) and glacial acetic acid

Table 2 Selected bond distances (Å) and angles (°) with estimated standard deviations in parentheses

cis-(L)$_2$PtCl$_2$ (**2**)			
Pt(1)–P(1)	2.260(4)	P(1)–C(14)	1.818(12)
Pt(1)–Cl(1)	2.365(4)	N(1)–C(9)	1.367(17)
P(1)–C(1)	1.892(13)	N(1)–C(2)	1.454(17)
P(1)–C(20)	1.801(14)	N(1)–C(1)	1.458(17)
P(1)–Pt(1)–P(1A)	97.78(18)	C(1)–P(1)–Pt(1)	112.2(5)
P(1)–Pt(1)–Cl(1A)	88.13(14)	C(9)–N(1)–C(2)	121.7(11)
P(1A)–Pt(1)–Cl(1A)	169.61(13)	C(9)–N(1)–C(1)	122.2(11)
P(1)–Pt(1)–Cl(1)	169.61(13)	C(2)–N(1)–C(1)	115.8(11)
P(1A)–Pt(1)–Cl(1)	88.13(14)	N(1)–C(1)–P(1)	114.1(10)
Cl(1A)–Pt(1)–Cl(1)	87.4(2)	N(1)–C(2)–C(3)	115.0(12)
trans-(L)$_2$Pt(C≡CPh)$_2$ (**3**)			
Pt(1)–C(26)	2.015(8)	N(1)–C(19)	1.422(16)
Pt(1)–P(1)	2.3039(19)	N(1)–C(13)	1.435(12)
P(1)–C(13)	1.885(7)	C(26)–C(27)	1.176(10)
N(1)–C(14)	1.397(14)	C(27)–C(28)	1.454(10)
C(26)–Pt(1)–C(26A)	180.0(5)	C(14)–N(1)–C(19)	122.9(10)
C(26)–Pt(1)–P(1)	91.9(2)	C(14)–N(1)–C(13)	118.7(8)
C(26A)–Pt(1)–P(1)	88.1(2)	C(19)–N(1)–C(13)	118.0(10)
C(26)–Pt(1)–P(1A)	88.1(2)	N(1)–C(13)–P(1)	113.5(6)
C(26A)–Pt(1)–P(1A)	91.9(2)	N(1)–C(19)–C(20)	116.3(10)
P(1)–Pt(1)–P(1A)	180.00(10)	C(27)–C(26)–Pt(1)	179.0(7)
C(13)–P(1)–Pt(1)	116.0(3)	C(26)–C(27)–C(28)	176.7(9)
PtCu$_2$(L)$_2$(C≡CPh)$_2$(H$_2$O)$_2$(ClO$_4$)$_2$ (**4′**)			
Cu(1)–C(26)	2.003(7)	Pt(1)–P(1)	2.306(2)
Cu(1)–C(27)	2.005(7)	P(1)–C(13)	1.892(8)
Cu(1)–N(2)	2.016(6)	N(1)–C(13)	1.453(9)
Cu(1)–O(5)	2.038(7)	C(26)–C(27)	1.238(10)
Pt(1)–C(26)	2.003(8)	C(27)–C(28)	1.463(10)
C(26)–Cu(1)–C(27)	36.0(3)	C(13)–P(1)–Pt(1)	120.9(3)
C(26)–Cu(1)–N(2)	111.9(3)	C(8)–N(1)–C(13)	122.7(6)
C(27)–Cu(1)–N(2)	147.9(3)	C(8)–N(2)–Cu(1)	127.3(6)
C(26)–Cu(1)–O(5)	152.3(3)	C(12)–N(2)–Cu(1)	109.5(6)
C(27)–Cu(1)–O(5)	118.1(3)	N(2)–C(8)–N(1)	117.2(7)
N(2)–Cu(1)–O(5)	93.7(3)	N(1)–C(13)–P(1)	114.1(5)
C(26A)–Pt(1)–C(26)	180.0(4)	C(27)–C(26)–Pt(1)	174.4(7)
C(26A)–Pt(1)–P(1)	88.4(2)	C(27)–C(26)–Cu(1)	72.1(5)
C(26)–Pt(1)–P(1)	91.6(2)	Pt(1)–C(26)–Cu(1)	113.4(4)
C(26A)–Pt(1)–P(1A)	91.6(2)	C(26)–C(27)–C(28)	163.1(8)
C(26)–Pt(1)–P(1A)	88.4(2)	C(26)–C(27)–Cu(1)	71.9(5)
P(1)–Pt(1)–P(1A)	180.0	C(28)–C(27)–Cu(1)	124.9(6)
PtCu$_2$(L)$_2$(C≡CPh)$_2$(CH$_3$CN)$_2$(ClO$_4$)$_2$·CH$_2$Cl$_2$ (**4″**·CH$_2$Cl$_2$)			
Pt(1)–C(26)	2.024(8)	Cu(1)–C(26)	2.030(8)
Pt(1)–P(1)	2.324(2)	P(1)–C(13)	1.897(11)
Cu(1)–N(3)	1.965(9)	N(1)–C(13)	1.414(12)
Cu(1)–N(2)	2.018(9)	C(1)–C(2)	1.532(16)
Cu(1)–C(27)	2.020(10)	C(26)–C(27)	1.249(11)
C(26A)–Pt(1)–C(26)	180.000(1)	C(27)–Cu(1)–C(26)	35.9(3)
C(26A)–Pt(1)–P(1)	88.2(2)	C(13)–P(1)–Pt(1)	111.8(3)
C(26)–Pt(1)–P(1)	91.8(2)	C(8)–N(1)–C(13)	121.3(9)
C(26A)–Pt(1)–P(1A)	91.8(2)	N(2)–C(8)–N(1)	119.5(10)
C(26)–Pt(1)–P(1A)	88.2(2)	N(1)–C(13)–P(1)	115.0(7)
P(1)–Pt(1)–P(1A)	180.00(13)	C(27)–C(26)–Pt(1)	166.7(8)
N(3)–Cu(1)–N(2)	99.0(4)	C(27)–C(26)–Cu(1)	71.6(6)
N(3)–Cu(1)–C(27)	116.6(4)	Pt(1)–C(26)–Cu(1)	119.8(4)
N(2)–Cu(1)–C(27)	144.1(3)	C(26)–C(27)–C(28)	158.4(10)
N(3)–Cu(1)–C(26)	152.0(4)	C(26)–C(27)–Cu(1)	72.5(6)
N(2)–Cu(1)–C(26)	108.9(3)	C(28)–C(27)–Cu(1)	128.2(6)

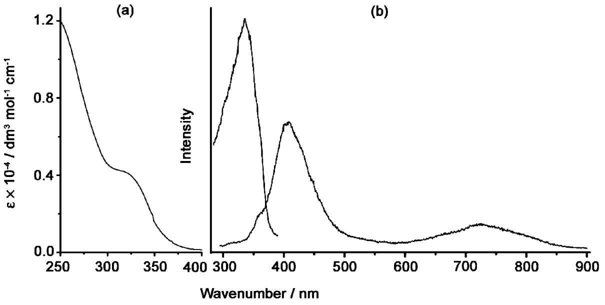

Fig. 5 The absorption spectra (a), the excitation spectra ($\lambda_{monitor}$ = 408 nm) and the fluorescence emission spectra (λ_{ex} = 323 nm) (b) of the trinuclear complex **4** in CH$_2$Cl$_2$ solution (concentration, 1 × 10^{-5} M).

(2.40 g, 2.4 ml, 40 mmol) in toluene (50 ml), Ph$_2$PH (3.72 g, 3.4 ml, 20 mmol) was added dropwise with stirring at 70–80 °C. The mixture was reacted at 70–80 °C until all of paraformaldehyde had completely disappeared (about 6 h). After cooling the solvent was removed under vacuum and the residue was dissolved in 100 ml CH$_2$Cl$_2$. A solution of 2.0 g NaOH in 100 ml water was added to neutralize the acid. Then the organic phase was separated and dried with anhydrous MgSO$_4$. After removing the CH$_2$Cl$_2$ in vacuum, the crude product was obtained and recrystallized from CH$_2$Cl$_2$–CH$_3$OH to give 6.58 g (86%) of ligand **1** as a white solid powder, mp 83–84 °C. Anal. Calc. for C$_{25}$H$_{23}$N$_2$P: C, 78.51; H, 6.06; N, 7.32. Found: C, 78.45; H, 6.14, N, 7.48%. ^{1}H NMR (CDCl$_3$): 4.45 (s, 2H, CH$_2$ in benzyl), 5.12 (s, 2H, NCH$_2$P), 6.23 (t, 2H, 4′ and 5′-CH in pyridinyl), 6.79 (d, 1H, 3′-CH in pyridinyl), 7.01–7.51 (m, 15H, C$_6$H$_5$), 7.82 (d, 1H, 6′-CH in pyridinyl) ppm. ^{31}P NMR (CDCl$_3$): −21.62 (s) ppm.

Preparation of *cis*-(L)$_2$PtCl$_2$ (2)

A mixture of 0.374 g Pt(COD)Cl$_2$ (1.0 mmol) and 0.764 g of ligand **1** (2.0 mmol) in CH$_2$Cl$_2$ (50 ml) was stirred for 2 h at room temperature. The mixture was filtered and the solvent was concentrated to a small volume and diethyl ether was subsequently added to the solution to give 0.94 g (91%) of **2** as an air-stable white solid, mp 230–232 °C. The sample for analysis was further purified by recrystallization from CH$_2$Cl$_2$–*n*-hexane. Anal. Calc. for C$_{50}$H$_{46}$N$_4$P$_2$PtCl$_2$: C, 58.26; H, 4.50; N, 5.43. Found: C, 57.99; H, 4.35; N, 5.25%. ^{1}H NMR (CDCl$_3$): 4.41 (s, 4H, CH$_2$ in benzyl), 5.02 (s, 4H, NCH$_2$P), 6.53 (t, 4H, 4′- and 5′-CH in pyridinyl), 6.70 (d, 2H, 3′-CH in pyridinyl), 7.01–7.06 (m, 10H, C$_6$H$_5$ in benzyl), 7.20–7.44 (m, 20H, P(C$_6$H$_5$)$_2$), 7.99 (d, 2H, 6′-CH in pyridinyl) ppm. ^{31}P NMR (CDCl$_3$): 6.04 (t) ppm, J_{Pt-P} = 3700 Hz.

Preparation of *trans*-(L)$_2$Pt(C≡CPh)$_2$ (3)

(a) From the reaction of the ligand L with (COD)Pt(C≡CPh)$_2$. A mixture of 0.505 g (COD)Pt(C≡CPh)$_2$ (1.0 mmol) and 0.764 g ligand **1** (2.0 mmol) in CH$_2$Cl$_2$ (50 ml) was stirred for 1 h at room temperature. The mixture was filtered and the solvent was concentrated to a small volume and diethyl ether was subsequently added to the solution to give 0.98 g (85%) of **3** as an air-stable white solid, mp 187–188 °C. The sample for analysis was further purified by recrystallization from CH$_2$Cl$_2$–Et$_2$O. Anal. Calc. for C$_{66}$H$_{56}$N$_4$P$_2$Pt: C, 68.21; H, 4.86; N, 4.82. Found: C, 68.09; H, 4.94; N, 4.97%. FT-IR (KBr, disk): *ν*(C≡C) 2107.6 (vs) cm^{-1}. ^{1}H NMR (CDCl$_3$): 4.94 (s, 4H, CH$_2$ in benzyl), 5.50 (s, 4H, NCH$_2$P), 6.33 (t, 4H, 4′- and 5′-CH in pyridinyl), 6.86 (d, 2H, 3′-CH in pyridinyl), 7.01–7.89 (m, 40H, C$_6$H$_5$), 7.92 (d, 2H, 6′-CH in pyridinyl) ppm. ^{31}P NMR (CDCl$_3$): 4.44 (t) ppm, J_{Pt-P} = 2478 Hz.

(b) From the reaction of *cis*-(L)$_2$PtCl$_2$ (2) with NaC≡CPh. A solution of phenylacetylene (0.12 ml, 0.11 g, 1.1 mmol) in 5 ml anhydrous ethanol was added dropwise to a solution of NaOC$_2$H$_5$ (1.2 mmol, 1 mmol ml^{-1}) in anhydrous C$_2$H$_5$OH (5 ml). The mixture was reacted for 10 min and was transferred to a suspension of *cis*-(L)$_2$PtCl$_2$ (0.516 g, 0.5 mmol) in 20 ml of anhydrous EtOH. The mixture was reacted for 8 h at room temperature. After removing the solvents in vacuum, the residue was extracted with 150 ml CH$_2$Cl$_2$–H$_2$O (1 : 2). The organic phase was separated and dried with anhydrous MgSO$_4$. After removing the CH$_2$Cl$_2$ in vacuum, the crude product was recrystallized from CH$_2$Cl$_2$–CH$_3$OH to give 0.27 g (46%) of **3**.

Table 3 Comparison of some bond lengths and angles in **3**, **4′** and **4″**·CH_2Cl_2 with those in structure-similar Pt–Cu complexes containing μ-η^1,η^2-C≡CPh

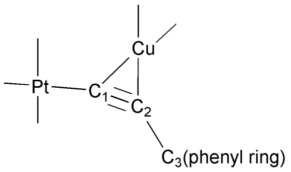

	Bond distances/Å			Bond angles/°	
	Pt–C_1	Cu–C_1, Cu–C_2	C_1≡C_2	Pt–C_1–C_2	C_1–C_2–C_3
[*trans*-$(L)_2Pt(C≡CPh)_2$], **3**	2.015(8)		1.176(10)	179.0(7)	176.7(9)
[Pt(μ–L)$_2$(C≡CPh)$_2$[Cu(H$_2$O)]$_2$(ClO$_4$)$_2$], **4′**	2.003(8)	2.003(7), 2.005(7)	1.238(10)	174.4(7)	163.1(8)
[Pt(μ-L)$_2$(C≡CPh)$_2$[Cu(CH$_3$CN)]$_2$(ClO$_4$)$_2$], **4″**[b]	2.024(8)	2.03(8), 2.02(10)	1.249(11)	166.7(8)	158.4(10)
[Pt$_2$(μ-dppm)$_2$(C≡CPh)$_4${Cu(CH$_3$CN)}$_2$]$^{2+}$, **A**[5][a]	2.02(1)	2.12(1), 2.10(4)	1.20(2)	164.8(10)	167.0(1)
[Pt(μ-dppy)$_2$(C≡CPh)$_2${Cu(CH$_3$CN)$_2$}$_2$]$^{2+}$, **B**[6][b]	2.002(4)	2.101(4), 2.173(3)	1.212(6)	177.7(3)	169.5(3)
[Pt(bipy)(C≡CPh)$_2$CuBr], **C**[7][c]	1.996(5)	1.193(5), 2.328(5)	1.207(6)	172.2(5)	166.1(5)
[Pt(^{t}Bu$_2$bipy)(C≡CC$_6$H$_4$Me-*p*)$_2$Cu(SCN)], **D**[8][d]	1.971(12)	2.156(11), 2.254(11)	1.24(2)	175.5(9)	162.8(11)

[a] dppm = Bis(diphenylphosphine)methane. [b] dppy = 2-Diphenylphosphinopyridine. [c] bipy = 2,2′-Bipyridine. [d] ^{t}Bu$_2$bipy = 4,4′-Bis-*tert*-2,2′-bipyridine.

Table 4 Absorption and emission data for complexes **3**, **4** and **5**[a]

	Absorption λ/nm (ε_{max}/dm^3 mol^{-1} cm^{-1})	Emission λ/nm
3	252 (16 700), 312 (7480)	408
4	249 (12 100), 323 (4060)	408, 730
5	245 (9600), 319 (3600)	385, 740

[a] The absorption spectra and fluorescence emission spectra were recorded with a concentration of 1 × 10^{-5} M in dichloromethane at room temperature.

Preparation of $PtCu_2(L)_2(C≡CPh)_2(ClO_4)_2$ (4)

A mixture of 0.116 g **3** (0.1 mmol) and 0.066 g $Cu(CH_3CN)_4ClO_4$ (0.2 mmol) in CH_2Cl_2 (20 ml) was stirred for 0.5 h at room temperature to give a yellow solution. The mixture was filtered and the solvent was concentrated to a small volume and diethyl ether was subsequently added to the solution. The precipitate was filtered off and dried in vacuum to give 0.12 g (79%) of **4** as a pale yellow powder, mp 138 °C (decomp.). The sample for analysis was further purified by recrystallization from CH_2Cl_2–Et_2O. Anal. Calc. for **4**, $C_{66}H_{56}N_4P_2PtCu_2Cl_2O_8$: C, 53.27; H, 3.79; N, 3.76. Found: C, 53.25; H, 4.02; N, 3.83%. FT-IR (KBr, disk): ν(C≡C) 2127.0 (s) cm^{-1}. ^{31}P NMR ($CDCl_3$): 4.82 (t) ppm, $J_{Pt–P}$ = 2996 Hz. Another experiment was similarly proceeded using 0.116 g of **3** (0.1 mmol) and 0.066 g of $Cu(CH_3CN)_4ClO_4$ (0.2 mmol), but in a mixed solvent of CH_2Cl_2–CH_3CN (1 : 1), to give 0.11 g of **4** (74%).

Complex **4** was recrystallized from CH_2Cl_2–wet MeOH and CH_2Cl_2–CH_3CN, to give the solvent-coordinated heterometallic complexes Pt[Cu(H$_2$O)]$_2$(μ-L)$_2$(C≡CPh)$_2$(ClO$_4$)$_2$ (**4′**) and Pt[Cu(CH$_3$CN)]$_2$(μ-L)$_2$(C≡CPh)$_2$(ClO$_4$)$_2$ (**4″**·CH_2Cl_2), respectively. Crystals of complexes **4′** and **4″**·CH_2Cl_2 suitable for X-ray structural analysis were easily grown by the slow evaporation of the corresponding solution of the complex in CH_2Cl_2–wet MeOH and CH_2Cl_2–CH_3CN, respectively.

Preparation of $PtAg_2(L)_2(C≡CPh)_2(ClO_4)_2$ (5)

A similar procedure, as described above, using 0.116 g of **3** (0.1 mmol) and 0.074 g of $Ag(CH_3CN)_4ClO_4$ (0.2 mmol) in CH_2Cl_2 (20 ml), gave 0.125 g (79%) of **5** as a yellow powder, mp 130 °C (decomp.). The sample for analysis was further purified by recrystallization from CH_2Cl_2–Et_2O. Anal. Calc. for $C_{66}H_{56}N_4P_2PtAg_2Cl_2O_8$: C, 50.27; H, 3.58; N, 3.55. Found: C, 50.15; H, 3.43; N, 3.25%. FT-IR (KBr, disk): ν(C≡C) 2119.0 (m) cm^{-1}. FAB-MS, *m*/*z*: 1573 (M$^+$), 1474 ([M − ClO$_4$]$^+$). ^{1}H NMR ($CDCl_3$): 4.21 (s, 4H, CH_2 in benzyl), 4.59 (s, 4H, NCH_2P), 6.65 (t, 4H, 4′- and 5′-CH in pyridinyl), 6.96 (d, 2H, 3′-CH in pyridinyl), 7.05–7.71 (m, 40H, C_6H_5), 7.74 (d, 2H, 6′-CH in pyridinyl) ppm. ^{31}P NMR ($CDCl_3$): 4.82 (t) ppm, $J_{Pt–P}$ = 2684 Hz.

Reaction of complex 4 with Na_2S

A solution of 0.048 g of $Na_2S·9H_2O$ (0.2 mmol) in 10 ml CH_3OH was added to a solution of 0.12 g **4** (0.072 mmol) in 10 ml CH_2Cl_2 with stirring and a black precipitate was produced immediately. The precipitate was filtered off and the solvent was removed under vacuum. The residue was recrystallized in CH_2Cl_2–diethyl ether to give complex **3** quantitatively.

A similar reaction for complex **5** can be undertaken to give **3** quantitatively.

X-Ray single-crystal structural determination of complexes

The X-ray quality crystal of complex **2**, **3**, **4′** and **4″**·CH_2Cl_2 was obtained by slow evaporation of its solution in CH_2Cl_2–hexane, CH_2Cl_2–MeOH, CH_2Cl_2–MeOH and CH_2Cl_2–MeCN, respectively. For each of complexes **2**, **3** and **4′**, a selected single crystal was mounted on a Bruker SMART 1000 CCD diffractometer operating at 50 kV and 30 mA using Mo-Kα radiation (0.71073 Å). For complex **4″**·CH_2Cl_2, the selected crystal was encapsulated in a double-sealed micro-tube and was mounted on the diffractometer. Data collection at 293 K and reduction were performed using the SMART and SAINT software,[14] with frames of 0.3° oscillation in the range $1.5 < \theta < 26°$ (for **4′**, $\theta < 24°$), An empirical absorption correction was applied using the SADABS program.[15] An empirical absorption correction was applied using ψ-scan data. The structures were solved by direct methods and all non-hydrogen atoms were subjected to anisotropic refinement by full-matrix least squares on F^2 using the SHELXTL package.[16] Non-hydrogen atoms were subjected to anisotropic refinement. All hydrogen atoms were generated geometrically (C–H bond lengths fixed at 0.96 Å), assigned appropriate isotropic thermal parameters and included in structure factor calculations. The crystal structure data and refinement details are summarized in Table 1.

CCDC reference numbers 197274–197277.

See http://www.rsc.org/suppdata/dt/b2/b211301p/ for crystallographic data in CIF or other electronic format.

Acknowledgements

We are grateful to the National Science Foundation of China for financial support of this research work (Project Grant No. 20102003).

References

1 See, for example: (*a*) Z. Z. Zhang and H. Cheng, *Coord. Chem. Rev.*, 1996, **147**, 1; (*b*) P. Espinet and K. Soulantica, *Coord. Chem. Rev.*, 1999, **193–195**, 499.

2 See, for example: (*a*) A. L. Balch, *Prog. Inorg. Chem.*, 1993, **41**, 239; (*b*) H. B. Song, Z. Z. Zhang, Z. Hui, M. C. Che and T. C. W. Mak, *Inorg. Chem.*, 2002, **41**, 3146; (*c*) H. B. Song, Z. Z. Zhang and T. C. W. Mak, *Inorg. Chem.*, 2001, **40**, 5928; (*d*) S. M. Kuang, Z. Z. Zhang, Q. G. Wang and T. C. W. Mak, *J. Chem. Soc., Dalton Trans.*, 1998, 2927; (*e*) H. B. Song, Q. M. Wang, Z. Z. Zhang and T. C. W. Mak, *J. Chem. Soc., Dalton Trans.*, 2001, 1658.

3 (*a*) S. E. Durrn, M. B. Smith, A. M. A. Shawin and J. W. Steed, *J. Chem. Soc., Dalton Trans.*, 2000, 2778; (*b*) H. B. Song, Z. Z. Zhang and T. C. W. Mak, *J. Chem. Soc., Dalton Trans.*, 2002, 1336.

4 (*a*) H. B. Song, Q. M. Wang, Z. Z. Zhang and T. C. W. Mak, *J. Organomet. Chem.*, 2000, **605**, 15; (*b*) H. B. Song, Z. Z. Zhang and T. C. W. Mak, *New. J. Chem.*, 2002, **26**, 113; (*c*) D. J. Cui, Q. S. Li, F. B. Xu, X. B. Leng, X. S. Zeng and Z. Z. Zhang, *Organometallics*, 2001, **20**, 4126.

5 V. W. W. Yam, K. L. Yu, K. M. C. Wong and K. K. Cheung, *Organometallics*, 2001, **20**, 721.

6 V. W. W. Yam, L. P. Chan and T. F. Lai, *J. Chem. Soc., Dalton Trans.*, 1993, 2075.

7 H. Lang, A. del Villar and G. Rheinwald, *J. Organomet. Chem.*, 1999, **587**, 284.

8 C. J. Adams and P. R. Raithby, *J. Organomet. Chem.*, 1999, **578**, 178.

9 V. W. W. Yam, K. K. W. Lo and K. M. C. Wong, *J. Organomet. Chem.*, 1999, **578**, 3.

10 O. Kemal and C. B. Reese, *J. Chem. Soc., Perkin Trans. 1*, 1981, **5**, 1569–73.

11 D. Drew and J. R. Doyle, *Inorg. Synth.*, 1972, **13**, 47.

12 (*a*) M. Herberhold, T. Schmalz, W. Milius and B. Wrackmeyer, *J. Organomet. Chem.*, 2002, **641**, 173–84; (*b*) R. J. Cross and M. F. Davidson, *J. Chem. Soc., Dalton Trans.*, 1986, 1987.

13 (*a*) W. C. Wolsey, *J. Chem. Educ.*, 1973, **50**, A335; (*b*) K. N. Raymond, *Chem. Eng. News*, 1983, **61**, 4.

14 SMART 5.0 and SAINT 4.0 for Windows NT, Area Detector Control and Integration Software, Bruker Analytical X-Ray Systems, Inc., Madison, WI, USA, 1998.

15 G. M. Sheldrick, SADABS, Program for Empirical Absorption Correction of Area Detector Data,University of Göttingen, Germany, 1996.

16 G. M. Sheldrick, SHELXTL 5.10 for Windows NT, Structure Determination Software Programs, Bruker Analytical X-Ray Systems, Inc., Madison, WI, USA, 1997.